Published in final edited form as:

Nature. 2010 June 17; 465(7300): 956–960. doi:10.1038/nature09080.

TFIIA and the transactivator Rap1 cooperate to commit TFIID for transcription initiation

Gabor Papai[1], **Manish K. Tripathi**[2], **Christine Ruhlmann**[1], **Justin H. Layer**[2], **P. Anthony Weil**[2], and **Patrick Schultz**[1,*]

[1]Department of Structural Biology and Genomics, Institut de Génétique et de Biologie Moléculaire et Cellulaire CNRS/INSERM/ULP, 1, rue Laurent Fries, BP10142, 67404 Illkirch, France

[2]Department of Molecular Physiology & Biophysics, Vanderbilt University, School of Medicine, Nashville, Tennessee 37232, USA

Abstract

Transcription of eukaryotic mRNA encoding genes by RNA polymerase II (Pol II) is triggered by the binding of transactivating proteins to enhancer DNA, which stimulates the recruitment of general transcription factors (GTFs; TFIIA, B, D, E, F, H) and Pol II on the cis-linked promoter leading to preinitiation complex (PIC) formation and transcription1. In TFIID-dependent activation pathways, this TATA box Binding Protein (TBP)-containing GTF is first recruited on the promoter through interaction with activators1-3 and cooperates with TFIIA to form a committed PIC4. However, neither the mechanisms by which activation signals are communicated between these factors, nor the structural organization of the activated PIC are known. Here we used cryo-electron microscopy to determine the architecture of nucleoprotein complexes composed of TFIID, TFIIA, the transcriptional activator Rap1 and yeast enhancer-promoter DNA. These structures revealed the mode of binding of Rap1 and TFIIA to TFIID, as well as a reorganization of TFIIA induced by its interaction with Rap1. We propose that this change in position increases the exposure of TBP within TFIID, consequently enhancing its ability to interact with the promoter. A large Rap1-dependent DNA loop forms between the activator binding site and the proximal promoter region, and this loop is topologically locked by a TFIIA-Rap1 protein bridge that folds over the DNA. These results highlight the role of TFIIA in transcriptional activation, define a molecular mechanism for enhancer-promoter communication and provide important new structural insights into the pathways of intramolecular communication that convey transcription activation signals through the TFIID complex.

*Corresponding Author: patrick.schultz@igbmc.u-strasbg.fr, Tel.: +33-388-655750 Fax: +33-388-653201.

Author contributions P.S. and P.A.W. initiated the study. M.K.T. purified the complexes and carried out the biochemical tests. J.H.L. participated in the design and production of mutant proteins. C.R. and G.P. performed the looping experiments. P.S. and G.P. prepared the samples for microscopy and recorded the images. G.P. performed the image analysis. The manuscript was prepared and commented by P.S., P.A.W., M.K.T. and G.P.

Author informations

The electron density maps of the hydrated TFIID, the TFIID-TFIIA-DNA complex and the TFIID-TFIIA-Rap1-DNA Complex I and Complex II were deposited in the EM Database under accession codes EM-5175, EM-5178, EM-5176 and EM-5177, respectively.

Three-dimensional (3-D) electron microscopy (EM) has provided structural models for yeast TFIID5,6 that bears close similarities with its human ortholog7,8. TFIID can be divided into five modules5,7, lobes A, B, C1, C2 and D that adopt a clamp-like structure in which lobes A and B form the jaws (Fig. 1a). TFIID serves as a coactivator for yeast transcription factor Rap1 through direct interactions with TFIID subunits Taf4, 5 and 12. The Rap1 transactivator was used here as a model to study the architecture of a DNA-bound activator-TFIID-TFIIA complex9. Rap1 is a multifunctional protein that plays important roles in gene transcription and telomere length regulation, acts both as a repressor or activator on different genes10, drives transcription of over 40% of Pol II transcription in yeast, and is essential for transcription of the ribosomal protein genes used here as a model9,11. In order to elucidate the architecture of an activator-TFIID-promoter DNA complex we assembled three TFIID-containing complexes and solved their molecular structure to a resolution of 18.6 - 35 Å, mostly by utilizing cryo-EM methods (supplementary Table 1).

To visualize the Rap1 binding site on TFIID we first analyzed the structure of the TFIID-Rap1 complex formed as described in Methods with five-fold molar excess of Rap1. The recorded image dataset was analyzed and ultimately separated into two species, Rap1-TFIID complex, and holo-TFIID (supplemental material). A comparison of the two resulting models revealed that while the TFIID-Rap1 complex contained an additional density, the binding of Rap1 did not induce major conformational changes in TFIID, in agreement with a recent report describing the interaction of human TFIID with activators12. The additional Rap1-dependent protein density is found in TFIID lobe B (Fig. 1b and Supplementary Fig. 5a) where it colocalizes with Taf5 and the Histone Fold Domain containing heterodimer Taf4/Taf12, consistent with our immunolabelling experiments8,13 and with Rap1-Taf binding studies9,14, thus we conclude that the extra mass in the TFIID-Rap1 complex corresponds to Rap1 binding with Tafs 4, 5 and 12.

In order to position TFIIA and TFIID-DNA interactions in the absence of activator we recorded cryo-EM images of a TFIID-TFIIA-DNA complex reconstituted on the Adenovirus 2 Major Late Promoter (Ad2 MLP)15 with forty-fold molar excess of TFIIA and four-fold molar excess of DNA. Upon refinement, the image dataset was sorted to remove free, non-DNA bound TFIID molecules thus yielding 3-D models for the TFIID-TFIIA-DNA complex and holo-TFIID (Fig. 1c and Supplementary Fig. 4a and 5b). In the TFIID-TFIIA-DNA complex an additional globular density was bound to lobe C1, which showed a rod-shaped extension towards lobe D. The globular density is compatible with the size of TFIIA and positions close to the mapped location of TBP13 consistent with the known TBP-TFIIA interaction16,17. The rod-shaped density connects to lobe D and runs along its surface where we have mapped the C-terminus of Taf2 (see Supplementary Fig. 7). Since Taf2 is documented to interact with the Inr sequence at the transcription start site in the Ad2 MLP18,19, we propose that the extra density depicted in green in Fig. 1c corresponds to promoter DNA. The additional mass present in the TFIIA-TFIID-DNA complex thus contains TFIIA and a promoter DNA fragment connecting TBP to Taf2.

We next incubated TFIID, TFIIA and Rap1 with a chimeric yeast enhancer-promoter DNA fragment composed of the 41 bp Rap1 Upstream Activating Sequence of the ribosomal protein gene *RPS8A* (UAS_{RAP1}) fused to the *PGK1* core promoter20; ***UAS_{RAP1}-PGK1***,

Supplementary Fig. 8), by using a ten-fold molar excess of the DNA fragment and five-fold excess of both TFIIA and Rap1. Importantly, this minimal construct which contains two Rap1 binding sites fused to the *PGK1* promoter, has been well characterized. Transcription of this construct is both TFIID- and Rap1-dependent in vivo and in vitro9,20. A large dataset of 110,000 images was collected, aligned and classified according to particle orientation. Substantial heterogeneity was observed for similarly oriented particles indicating that the dataset contained a mixed population of complexes. Therefore 3-D multivariate statistical analysis was applied to separate different TFIID complexes21. This method reveals three dominant structures termed Complexes I, II and III. Complex III corresponds to free, unbound holo-TFIID, and serves here as an internal reference structure (Supplementary Fig. 4c and 5c,d).

Complex I contains TFIID, Rap1 and enhancer promoter DNA and is characterized by two additional densities bound to both faces of Lobe B (red, Fig 2a) positioned similarly to Rap1 within the TFIID-Rap1 complex. Importantly, the shape of the inner density, closest to lobe C1, accommodates the crystal structure of the Rap1 DNA Binding Domain (DBD)22 (Fig. 2b). This observation, indicating that Rap1 DBD binds directly to Lobe B, is consistent with biochemical and genetic evidence demonstrating that this central domain of Rap1 (residues 361 to 596) interacts with TFIID9. Moreover, this density shows a rod-shaped protuberance running towards and contacting lobe C2 (Lobe C2, green in Fig. 2a). When the atomic structure of the Rap1-DBD-DNA complex22 is fitted into the inner density the orientation and position of DNA overlaps the protruding rod suggesting that the narrow density connecting Rap1 on lobe B to lobe C2 corresponds to promoter DNA downstream of the Rap1-binding site. The shape of the density bound to the external face of lobe B, opposite to lobe D, is different from that of the Rap1-DBD and there is no protruding rod that could account for bound DNA, suggesting that it corresponds to other domains of Rap1. The 92 kDa Rap1 consists of DNA bending, BRCT, DBD, toxicity (Tox), AD and silencing (SD) domains23. Among these, both the DBD and the C-terminal portions of Rap1 (containing Tox, AD and SD domains) interact directly with the holo-TFIID complex, indicating that the C-terminal domain of Rap1 likely contributes to the observed external density9. In a control experiment we examined the structure of isolated Rap1 molecules and found that they adopt a two-lobed horseshoe shaped structure, consistent in size and shape with the two densities found in lobe B (Supplementary Fig. 10). We can however not completely rule out the possibility that this second density corresponds to a second Rap1 molecule. In addition to Rap1, Complex I contains an extra density associated with TFIID domain D near the Taf2 site (Lobe D, green in Fig. 2a). A similar density was detected at the same location in the TFIID-TFIIA-DNA complex suggesting that this density corresponds to DNA bound to Taf2. Thus, in Complex I, TFIID appears to contact DNA through Rap1 and Taf2, but apparently not through TBP and TFIIA, since no extra density was detected in lobe C1. Taken together these data suggest that complex I may correspond to an initial “recruitment mode” of binding, where TFIID interacts with the promoter-bound activator in the absence of TFIIA.

Complex II, a quaternary complex containing TFIID, Rap1, TFIIA and enhancer promoter DNA, is characterized by a continuous density between TBP and the Rap1 binding sites that

bridges lobes C1 and B (Fig. 3a). This bridge is too large to be composed of DNA alone and therefore must also contain protein. We propose that the mass next to lobe C1 corresponds to TFIIA, as TFIIA binds to a similar site of TFIID in the TFIID-TFIIA-DNA complex, and because this extra mass accommodates the atomic structure of the TFIIA-TBP-DNA complex24 (Fig. 3b). Notably though, comparison of Complex II with the TFIID-TFIIA-DNA complex, indicates that the position of TFIIA is rotated 130° around its TFIID interaction site (Fig. 3c). The repositioning of TFIIA within Complex II brings it close enough to directly interact with the DBD of Rap1, which is located on the inner face of lobe B as in Complex I. The proposed position of the Rap1 DBD is supported by the docking of its atomic structure into the remaining part of the protein bridge (Fig. 3b). Interactions between activators and TFIIA have been described25-28 and in one case TFIIA was shown to be required to release TBP from DNA binding autoinhibition mediated by the N-terminal TAND domain of Taf129, whereas in the other instances TFIIA was described to stimulate activator dependent transcription by interacting with the activator, the situation we observe here in Complex II. This reorganization of TFIIA within the TFIID-activator-promoter complex likely affects the position and therefore the accessibility (and functionality) of TBP, contributing to both increased TFIID-promoter interaction, PIC formation, and ultimately initiation efficiency. The exact path of promoter DNA cannot be traced in Complex II, though several extra densities signal its position. A patch of density is found on the inner wall of the clamp between lobes C1 and D, and a second more robust density is located in lobe D as observed in both Complex I and the TFIID-TFIIA-DNA complex (Lobe D, green in Fig. 3a). We interpret these stretches of density to correspond to the bound promoter DNA between the TATA box that interacts with TBP and the DNA close to the transcription start site bound by Taf2.

The DNA between the TATA-box and the Rap1 binding sites was not detected, most likely because of the flexibility of this segment. The proposed arrangement of the Rap1 DBD and TBP/TFIIA complexes implies that the intervening DNA loops out away from TFIID. To test this hypothesis we formed complexes on the yeast enhancer-promoter DNA fragment with TFIID and TFIIA in the presence and absence of Rap1. The resulting complexes were visualized after platinum shadowing and clearly revealed loops of DNA protruding from TFIID (Fig. 3d). Rap1 plays an essential role in loop formation since in the absence of Rap1, loops were observed in less than 2% of the DNA-bound TFIID complexes, while when Rap1 was added, 35% of the DNA bound TFIID molecules had DNA loops. Similar Rap1-dependent loop formation is observed on the natural *RPS1A* gene (Supplementary Fig. 9). Moreover TFIIA mutants unaffected in TBP binding but showing impaired transcription show a reduced ability to form DNA loops (Supplementary Fig. 11 and 12). These observations demonstrate that the Rap1 activator favours the formation of DNA loops allowing communication with distant TFIID-bound promoter sequences.

We propose that Complexes I and II represent functional intermediates in the pathway leading to PIC formation. From the molecular snapshots we have captured we infer a possible mechanism for activated TFIID-TFIIA-DNA complex formation (Fig.4). In a first step, Rap1 interacts with its recognition element (Fig. 4a) and this Rap1-enhancer complex can simultaneously bind TFIID (Fig. 4b). In all complexes analyzed, the Taf2–containing D

lobe was found to interact with the DNA template indicating that in the absence of detectable interaction with TBP or TFIIA, the DNA fragment is already looped out between the Rap1-binding sites and the proximal promoter (Fig. 4c and Supplementary Fig. 12). Whereas the role of TFIIA in releasing TBP autoinhibition in basal transcription is well established, its contribution to activated transcription at the molecular level is less well understood. The discovery of a class of TFIIA mutants that stimulate TBP-DNA binding but fail to support activation favours a model in which TFIIA acts in two mechanistically distinct activation steps27 consistent with the structures reported here (Fig. 4c,d,e), where we propose that the action of the activator is mediated by a protein bridge between lobes B and C1 of TFIID through an interaction between TFIIA and the Rap1 DBD (Fig. 4d). Thus activator-induced repositioning of TFIIA, and probably of its interaction partner TBP, may affect the accessibility of the DNA binding surface of TBP thereby facilitating functional PIC formation and activation of transcription (Complex II, Fig. 4d). In addition our model predicts that the bridge closes over the TBP-bound DNA and topologically locks the proximal promoter DNA in the resulting clamp (Complex I to Complex II; Fig. 4c,d). Such a trapping process could result in an increased residence time of the promoter DNA within TFIID and participate in the activation mechanism. Collectively our results support a role for TFIID as an assembly platform that plays an active and important role in PIC formation and transcription. Our data provide new structural insights into how, Rap1 collaborating with TFIIA, transduces activating intramolecular signals within the TFIID coactivator complex that ultimately can lead to PIC formation. Further, the structures reported here highlight the complex network of protein-protein and protein-DNA interactions regulating activated transcription.

METHODS SUMMARY

HA- and TAP-TFIID were purified from *Saccharomyces cerevisiae* as described5,9,15. The TFIID-Rap1 complex was assembled from TAP-tagged TFIID and a 5-fold molar excess of Rap1. The sample was brought to a TFIID concentration of 30 μg/ml, crosslinked with 0.1% glutaraldehyde for 5 sec and mounted as described5. A transmission electron microscope (TEM, Philips CM120) equipped with a LaB_6 cathode and operating at 120 kV was used to collect images with a CCD camera (Model 794, Gatan, Pleasanton). The TFIID-TFIIA-DNA complex was assembled from TAP-tagged TFIID with a 40-fold molar excess of TFIIA and 4-fold molar excess of a 400 bp long Ad2 MLP fragment (Supplementary Fig. 4). The specimen was crosslinked and adsorbed on a thin carbon film sustained by a holey carbon grid and plunge-frozen into liquid ethane. Images were recorded on a cryo-TEM (FEI Tecnai F20) and were digitized as described5. To form the TFIID-TFIIA-Rap1-DNA complex, HA-tagged TFIID was incubated with a 10-fold molar excess of a 282 bp UAS_{RAP1}-*PGK1* DNA fragment (Supplementary Fig. 4)9 and a 5-fold excess of both TFIIA and Rap1. The specimen was prepared as for the TFIID-TFIIA-DNA complex and data was collected on a cryo-TEM (FEI Tecnai Polara) operating at 300 kV. Images were selected and processed as described earlier5. Resolution was estimated according to the half bit criterion30 and the final reconstructions were filtered accordingly. During refinement images of the TFIID-Rap1 and TFIID-TFIIA-DNA complexes were split into holo-TFIID and multicomponent complexes. Analysis of the TFIID-TFIIA-Rap1-DNA complex was

similar except for a 3-D multivariate statistical analysis and clustering step that was performed to separate distinct conformational states according to ref 24.

Supplementary Material

Refer to Web version on PubMed Central for supplementary material.

Acknowledgements

This work was supported by grants from the Institut National de la Santé et de la Recherche Médicale, the Centre National pour la Recherche Scientifique, the Association pour la Recherche sur le Cancer (ARC), the Fondation pour la recherche médicale (FRM), the european SPINE program, QLG2-CT-00988 (G.P., C.R., P.S.), and the National Institutes of Health (NIH GM52461; M.K.T., J.H.L. and P.A.W.).

Appendix

METHODS

Protein purification and DNA probes

HA_1-Taf1- and TAP-Taf1-tagged TFIID were purified from *Saccharomyces cerevisiae* as described previously5,15,31. Rap1 and TFIIA were expressed in *E. coli* and purified as described9,15,16. Two promoter-containing DNA fragments were used to form complexes. The TFIID-TFIIA-DNA complex was assembled on a 400 bp long fragment of the Ad2 MLP, while a 282 bp long UAS_{RAP1}-*PGK1* chimeric yeast promoter (Supplementary Fig. 4) was used for the assembly of the TFIID-TFIIA-Rap1-DNA complex. This promoter fragment contains the 41 bp UAS_{RAP1} element, derived from the ribosomal protein-encoding *RPS8A* gene (from −252 to −212), which contains two binding sites for Rap1 (CTT**TACATCCATACACC**CTCTTT**AACACCCTTACACT**TTTA; Rap binding sites bold, underlined) fused to the *PGK1* core promoter (−211 to +30)9,20,32.

Sample preparation and electron microscopy

The final concentration of TFIID used in the negative stain and cryo-EM experiments was 30 μg/ml and of 50 μg/ml respectively. The crosslinked samples were treated with 0.1% glutaraldehyde for 5 sec prior to adsorption on a thin carbon film. To assemble the TFIID-Rap1 complex Tap-tagged TFIID was incubated with a 5-fold molar excess of Rap1 for 30 min on ice in 20 mM HEPES pH 7.9, 250 mM NaCl, 1 mM DTT, 0.2 mM PMSF and 10% glycerol. The sample was adsorbed onto air glow-discharged grids covered with a 10 nm thick carbon film and sandwiched with a second carbon film after negative staining with 2% uranyl acetate. A transmission electron microscope (TEM, Philips CM120) equipped with a LaB_6 cathode and operating at 120 kV was used to collect images at 45,000X magnification on a Pelletier-cooled slow scan CCD camera (Model 794, Gatan, Pleasanton, CA) resulting in a pixel spacing of 0.37 nm on the object. To assemble the TFIID-TFIIA-DNA complex, TAP-tagged TFIID was incubated for 20 min at 20°C with a 40-fold molar excess of TFIIA and 4-fold molar excess of the Ad2 MLP in 10 mM HEPES pH 7.4, 60 mM KCl, 6 mM $MgCl_2$ and 2 mM DTT. The specimen was adsorbed on a holey carbon grid covered with a 3-4 nm thick carbon film. Images were recorded on a cryo-TEM (FEI Tecnai F20) equipped with a field emission gun (FEG) and operating at 200 kV. Images of well dispersed

individual complexes were recorded at liquid nitrogen temperature on Kodak SO-163 films at 40,000 X magnification and in low dose conditions (15-20 e-/Å^2). Negatives were digitized with a 5 μm raster size using a drum scanner (Primescan D7100, Heidelberg) and were coarsened twice to obtain a pixel spacing of 0.254 nm on the object. For the TFIID-TFIIA-Rap1-DNA complex, HA-tagged TFIID was incubated 30 min at 20 °C with a 10-fold molar excess of *UAS$_{RAP1}$-PGK1* enhancer-promoter DNA, a 5-fold excess of TFIIA and a 5-fold excess of Rap1 in 10 mM Tris-HCl pH 7.9, 170 mM KOAc and 5 mM $MgCl_2$. The specimen prepared as detailed above for the TFIID-TFIIA-DNA complex, was vitrified in Vitrobot (FEI) and observed with a cryo-TEM (FEI Tecnai Polara) equipped with a FEG (field emission gun) operating at 300 kV. Images were collected at liquid nitrogen temperature under low-dose condition (15-20 e/Å^2), at a magnification of 39,000 X on Kodak SO-163 films. The pixel spacing of the digitized negatives was of 0.26 nm.

DNA loop formation was visualized after absorption of the DNA-protein complexes onto air glow-discharged grids that were positively stained with uranyl-acetate and platinum shadowed after air-drying.

Image processing

Boxing of the images of the TFIID-Rap1 and TFIID-TFIIA-DNA complexes was performed with the EMAN software33 package whereas the images of TFIID-TFIIA-Rap1-DNA complex were selected with the boxer2 option of EMAN234. The contrast transfer function (CTF) of the microscope was estimated using Bsoft:Bshow35 and the images were corrected by phase flipping. Image processing was performed using the IMAGIC36 (Image Science Software, Berlin, Germany) and Spider37 software packages as described earlier5. The resolutions of the final reconstructions were estimated according to the intersection point of the half bit curve with the FSC curve (half bit criterion)30. The final reconstructions were filtered to the estimated resolution.

In order to improve specimen homogeneity, TFIID-containing complexes that did not contain Taf2 were removed from the dataset5. During refinement, images of the TFIID-Rap1 and TFIID-TFIIA-DNA complex were split into holo-TFIID and complex. To do so, images were sorted for their best cross-correlation with reprojections of either the mixed (holo-TFIID + complex) model or the holo-TFIID reference model. This separation was iterated several times and resulted in a progressive enrichment of the mixed model in TFIID-Rap1 or TFIID-TFIIA-DNA complexes. The analysis of TFIID-TFIIA-Rap1-DNA complex was similar except for a 3-D statistical analysis and clustering step that was performed to separate distinct conformational states according to ref 24. Briefly, a large number of 3-D models were reconstructed from a few randomly selected and pre-aligned class average images. This repertoire of 3-D models was subjected to multivariate statistical analysis and was clustered into groups corresponding to different conformations of the complex. The class-sum volumes, characteristic for each conformation, were used as references for subsequent refinement rounds. Fitting of atomic coordinates into EM density maps were performed using UCSF Chimera's fit in map tool38 and Sculptor39. Images were created with UCSF Chimera.

LITERATURE CITED

1. Burley SK, Roeder RG. Biochemistry and structural biology of transcription factor IID (TFIID). Annu Rev Biochem. 1996; 65:769–799. [PubMed: 8811195]
2. Verrijzer CP, Tjian R. TAFs mediate transcriptional activation and promoter selectivity. Trends Biochem Sci. 1996; 21:338–342. [PubMed: 8870497]
3. Jacq X, et al. Human TAFII30 is present in a distinct TFIID complex and is required for transcriptional activation by the estrogen receptor. Cell. 1994; 79:107–117. [PubMed: 7923369]
4. Lieberman PM, Berk AJ. A mechanism for TAFs in transcriptional activation: activation domain enhancement of TFIID-TFIIA--promoter DNA complex formation. Genes Dev. 1994; 8:995–1006. [PubMed: 7926793]
5. Papai G, et al. Mapping the initiator binding Taf2 subunit in the structure of hydrated yeast TFIID. Structure. 2009; 17:363–373. [PubMed: 19278651]
6. Elmlund H, et al. Cryo-EM reveals promoter DNA binding and conformational flexibility of the general transcription factor TFIID. Structure. 2009; 17:1442–1452. [PubMed: 19913479]
7. Grob P, et al. Cryo-electron microscopy studies of human TFIID: conformational breathing in the integration of gene regulatory cues. Structure. 2006; 14:511–520. [PubMed: 16531235]
8. Leurent C, et al. Mapping histone fold TAFs within yeast TFIID. Embo J. 2002; 21:3424–3433. [PubMed: 12093743]
9. Garbett KA, Tripathi MK, Cencki B, Layer JH, Weil PA. Yeast TFIID serves as a coactivator for Rap1p by direct protein-protein interaction. Mol Cell Biol. 2007; 27:297–311. [PubMed: 17074814]
10. Sussel L, Shore D. Separation of transcriptional activation and silencing functions of the RAP1-encoded repressor/activator protein 1: isolation of viable mutants affecting both silencing and telomere length. Proc Natl Acad Sci U S A. 1991; 88:7749–7753. [PubMed: 1881914]
11. Lieb JD, Liu X, Botstein D, Brown PO. Promoter-specific binding of Rap1 revealed by genome-wide maps of protein-DNA association. Nat Genet. 2001; 28:327–334. [PubMed: 11455386]
12. Liu WL, et al. Structures of three distinct activator-TFIID complexes. Genes Dev. 2009; 23:1510–1521. [PubMed: 19571180]
13. Leurent C, et al. Mapping key functional sites within yeast TFIID. Embo J. 2004; 23:719–727. [PubMed: 14765106]
14. Layer JH, Miller SG, Weil PA. Direct transactivator-TFIID contacts drive yeast ribosomal protein gene transcription. J Biol Chem. 2010; 285 in press.
15. Sanders SL, Garbett KA, Weil PA. Molecular characterization of Saccharomyces cerevisiae TFIID. Mol Cell Biol. 2002; 22:6000–6013. [PubMed: 12138208]
16. Tan S, Hunziker Y, Sargent DF, Richmond TJ. Crystal structure of a yeast TFIIA/TBP/DNA complex. Nature. 1996; 381:127–151. [PubMed: 8610010]
17. Geiger JH, Hahn S, Lee S, Sigler PB. Crystal structure of the yeast TFIIA/TBP/DNA complex. Science. 1996; 272:830–836. [PubMed: 8629014]
18. Oelgeschlager T, Chiang CM, Roeder RG. Topology and reorganization of a human TFIID-promoter complex. Nature. 1996; 382:735–738. [PubMed: 8751448]
19. Chalkley GE, Verrijzer CP. DNA binding site selection by RNA polymerase II TAFs: a TAF(II)250-TAF(II)150 complex recognizes the initiator. Embo J. 1999; 18:4835–4845. [PubMed: 10469661]
20. Mencia M, Moqtaderi Z, Geisberg JV, Kuras L, Struhl K. Activator-specific recruitment of TFIID and regulation of ribosomal protein genes in yeast. Mol Cell. 2002; 9:823–833. [PubMed: 11983173]
21. Simonetti A, et al. Structure of the 30S translation initiation complex. Nature. 2008; 455:416–420. [PubMed: 18758445]
22. Konig P, Giraldo R, Chapman L, Rhodes D. The crystal structure of the DNA-binding domain of yeast RAP1 in complex with telomeric DNA. Cell. 1996; 85:125–136. [PubMed: 8620531]
23. Morse RH. RAP, RAP, open up! New wrinkles for RAP1 in yeast. Trends Genet. 2000; 16:51–53. [PubMed: 10652526]

24. Bleichenbacher M, Tan S, Richmond TJ. Novel interactions between the components of human and yeast TFIIA/TBP/DNA complexes. J Mol Biol. 2003; 332:783–793. [PubMed: 12972251]
25. Wang W, Gralla JD, Carey M. The acidic activator GAL4-AH can stimulate polymerase II transcription by promoting assembly of a closed complex requiring TFIID and TFIIA. Genes Dev. 1992; 6:1716–1727. [PubMed: 1516830]
26. Lieberman PM, Ozer J, Gursel DB. Requirement for transcription factor IIA (TFIIA)-TFIID recruitment by an activator depends on promoter structure and template competition. Mol Cell Biol. 1997; 17:6624–6632. [PubMed: 9343426]
27. Ozer J, Bolden AH, Lieberman PM. Transcription factor IIA mutations show activator-specific defects and reveal a IIA function distinct from stimulation of TBP-DNA binding. J Biol Chem. 1996; 271:11182–11190. [PubMed: 8626665]
28. Shykind BM, Kim J, Sharp PA. Activation of the TFIID-TFIIA complex with HMG-2. Genes Dev. 1995; 9:1354–1365. [PubMed: 7797075]
29. Kokubo T, Swanson MJ, Nishikawa JI, Hinnebusch AG, Nakatani Y. The yeast TAF145 inhibitory domain and TFIIA competitively bind to TATA-binding protein. Mol Cell Biol. 1998; 18:1003–1012. [PubMed: 9447997]
30. van Heel M, Schatz M. Fourier shell correlation threshold criteria. J Struct Biol. 2005; 151:250–262. [PubMed: 16125414]
31. Sanders SL, Weil PA. Identification of two novel TAF subunits of the yeast Saccharomyces cerevisiae TFIID complex. J Biol Chem. 2000; 275:13895–13900. [PubMed: 10788514]
32. Rathjen J, Mellor J. Characterisation of sequences required for RNA initiation from the PGK promoter of Saccharomyces cerevisiae. Nucleic Acids Res. 1990; 18:3219–3225. [PubMed: 2192358]
33. Ludtke SJ, Baldwin PR, Chiu W. EMAN: semiautomated software for high-resolution single-particle reconstructions. J Struct Biol. 1999; 128:82–97. [PubMed: 10600563]
34. Tang G, et al. EMAN2: an extensible image processing suite for electron microscopy. J Struct Biol. 2007; 157:38–46. [PubMed: 16859925]
35. Heymann JB. Bsoft: image and molecular processing in electron microscopy. J Struct Biol. 2001; 133:156–169. [PubMed: 11472087]
36. van Heel M, Harauz G, Orlova EV, Schmidt R, Schatz M. A new generation of the IMAGIC image processing system. J Struct Biol. 1996; 116:17–24. [PubMed: 8742718]
37. Frank J, et al. SPIDER and WEB: processing and visualization of images in 3D electron microscopy and related fields. J Struct Biol. 1996; 116:190–199. [PubMed: 8742743]
38. Pettersen EF, et al. UCSF Chimera--a visualization system for exploratory research and analysis. J Comput Chem. 2004; 25:1605–1612. [PubMed: 15264254]
39. http://sculptor.biomachina.org/

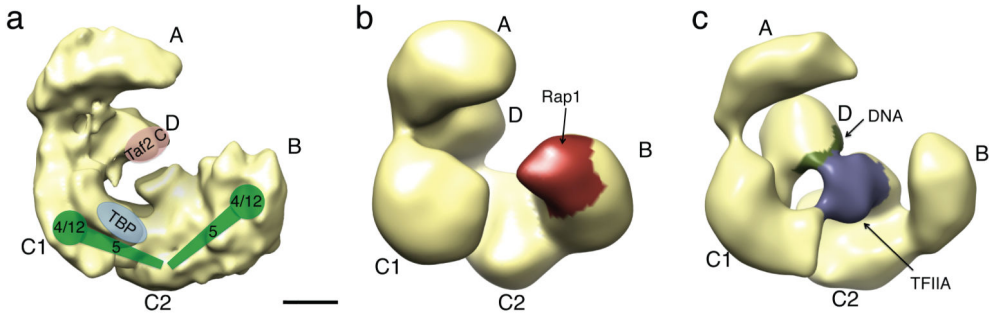

Figure 1. Location of critical components of the initiation process within various TFIID complexes

a, Cryo-EM structure of the yeast holo-TFIID complex. The five major lobes (A, B, C1, C2 and D)5,7 are depicted along with the location of TBP, Taf4, 5 and 12. Taf5 and the histone-fold Tafs, including Taf4 and Taf12, are present in two copies in yeast TFIID8,15 forming a crescent-shaped complex with two-fold symmetry5. **b**, Negatively stained structure of the TFIID-Rap1 complex. The additional density corresponding to Rap1 is colored in red according to difference maps shown in Supplementary Fig. 5a. **c**, Cryo-EM model of the unstained TFIID-TFIIA-DNA complex formed between TFIID, TFIIA and the Ad2 MLP. Additional densities present in the TFIID-TFIIA-DNA complex are colored. The mass corresponding to TFIIA is represented in blue whereas the density arising in the D lobe ascribed to DNA is represented in green. Original density difference maps are found in Supplementary Fig. 5b.

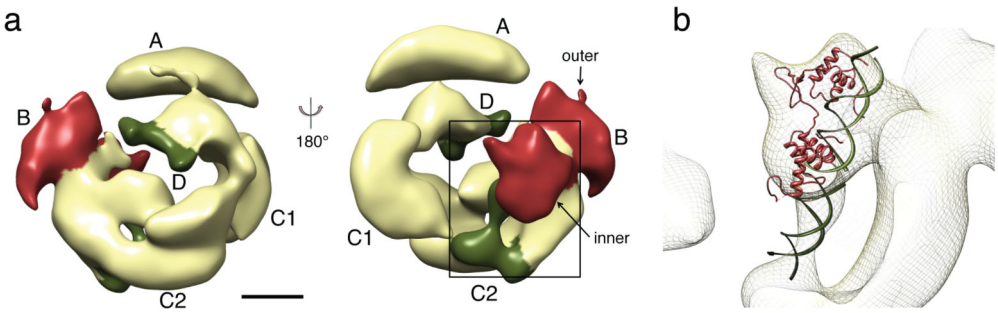

Figure 2. Structure of the initial TFIID-Activator-Promoter recruitment complex

a, Two different surface views of the Cryo-EM map of Complex I formed upon incubating TFIID, TFIIA, Rap1 and the *UAS_{RAP1}-PGK1* enhancer-promoter DNA. TFIIA is not detected in Complex I. Densities originating from Rap1 are detected on both sides of lobe B and are colored red. Densities attributed to DNA are colored green in lobes D and C2. **b**, Enlargement of the area boxed in (a) and fitting of the atomic model of DNA-bound Rap1 DBD into the additional Rap1-density contacting the inner face of lobe B. The rod of additional density protruding towards lobe C2 superimposes to the expected position of Rap1-bound DNA.

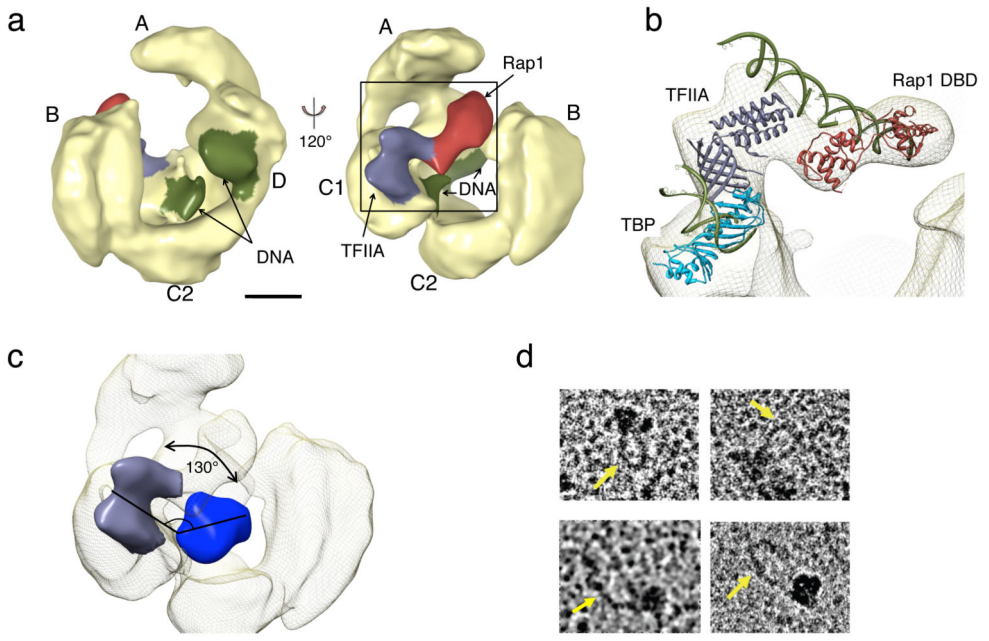

Figure 3. Structure of the committed complex

a, Two different surface views of the Cryo-EM map of Complex II formed upon incubating TFIID, TFIIA, Rap1 and *UAS$_{RAP1}$-PGK1* enhancer-promoter DNA. The additional densities revealed in Complex II are colored as follows: DNA, TFIIA and Rap1 are depicted in green, violet and red, respectively. **b**, Enlargement with slight tilting of the area boxed in (a) and fitting of the crystal structure of the TBP-TFIIA and the Rap1-DBD-DNA complexes identifies the bridging density between lobes C1 and B. Note that part of TFIIA is missing in the crystal structure and may affect the fitting **c**, Comparison of the position of TFIIA between the TFIID-TFIIA-DNA complex (blue) and Complex II (violet) reveals that the position of TFIIA is rotated by 130°. **d**, Platinum shadowing of spread TFIID-TFIIA-Rap1-DNA complexes showing the formation of a DNA loop in the presence of Rap1.

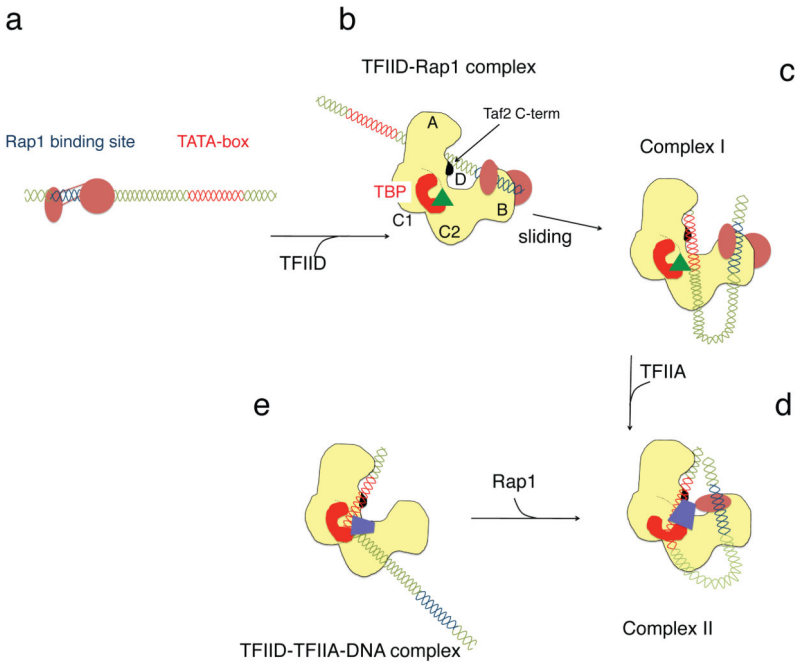

Figure 4. Model depicting the formation of the activated TFIID complex

a, Binding of Rap1 (red circles) to its specific DNA recognition elements. **b**, Recruitment of TFIID (yellow) through an interaction with Rap1 and Taf2 (black dot). **c**, Formation of a DNA loop. **d**, Recruitment of TFIIA (blue trapezoid) which induces the formation of a protein bridge between lobes B and C1 that locks the DNA loop. **e**, Model showing the different position of TFIIA in the TFIID-TFIIA-Ad2 MLP DNA complex, which naturally lacks Rap1.

The red shape corresponds to TBP while the green triangle represents TAND autoinhibition.